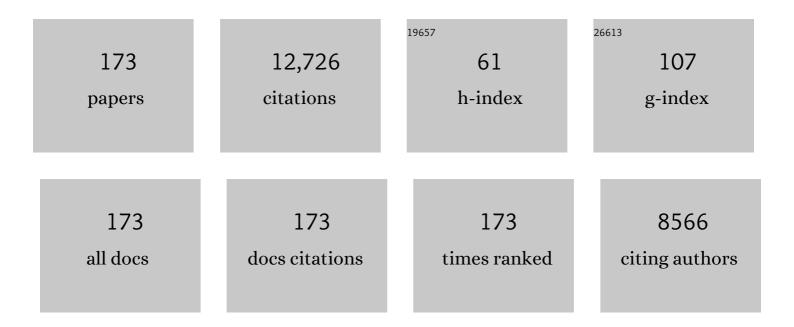
List of Publications by Year in descending order

Source: https://exaly.com/author-pdf/7122589/publications.pdf Version: 2024-02-01



#	Article	IF	CITATIONS
1	Highly enhanced microwave absorption for carbon nanotube/barium ferrite composite with ultra-low carbon nanotube loading. Journal of Materials Science and Technology, 2022, 102, 115-122.	10.7	37
2	Building of multifunctional and hierarchical HxMoO3/PNIPAM hydrogel for high-efficiency solar vapor generation. Green Energy and Environment, 2022, 7, 1006-1013.	8.7	21
3	Programmable micropatterned surface for single-layer homogeneous-polymer Janus actuator. Chemical Engineering Journal, 2022, 430, 133052.	12.7	23
4	Facile fabrication of highly durable superhydrophobic strain sensors for subtle human motion detection. Journal of Materials Science and Technology, 2022, 110, 35-42.	10.7	17
5	Preparation of <scp>PVA</scp> / <scp>PAM</scp> /Ag strain sensor via compound gelation. Journal of Applied Polymer Science, 2022, 139, 51883.	2.6	8
6	Polymer microfibrillar tube for continuous oil/water separation and collection. Polymer, 2022, 239, 124440.	3.8	8
7	Stretchable, Sensitive Strain Sensors with a Wide Workable Range and Low Detection Limit for Wearable Electronic Skins. ACS Applied Materials & Interfaces, 2022, 14, 4562-4570.	8.0	35
8	Preparation of wearable strain sensor based on PVA/MWCNTs hydrogel composite. Materials Today Communications, 2022, 31, 103278.	1.9	5
9	Farmingâ€Inspired Continuous Fabrication of Grating Flexible Transparent Film with Anisotropic Conductivity. Advanced Materials Technologies, 2022, 7, .	5.8	4
10	Hierarchical nanofibrous mat via water-assisted electrospinning for self-powered ultrasensitive vibration sensors. Nano Energy, 2022, 97, 107149.	16.0	24
11	Dynamic chemical bonds design strategy for fabricating fast room-temperature healable dielectric elastomer with significantly improved actuation performance. Chemical Engineering Journal, 2022, 439, 135683.	12.7	16
12	Sandwiched film with reversibly switchable transparency through cyclic melting-crystallization. Chemical Engineering Journal, 2022, 442, 136205.	12.7	12
13	Face-to-Face Assembly of Ag Nanoplates on Filter Papers for Pesticide Detection by Surface-Enhanced Raman Spectroscopy. Nanomaterials, 2022, 12, 1398.	4.1	9
14	Interface and electronic structure engineering induced Prussian blue analogues with ultra-stable capability for aqueous NH ₄ ⁺ storage. Nanoscale, 2022, 14, 8501-8509.	5.6	35
15	Dual-functional thermal management materials for highly thermal conduction and effectively heat generation. Composites Part B: Engineering, 2022, 242, 110084.	12.0	27
16	Multi-stimuli-responsive actuator based on bilayered thermoplastic film. Soft Matter, 2022, 18, 5052-5059.	2.7	8
17	Multifunctional interlocked e-skin based on elastic micropattern array facilely prepared by hot-air-gun. Chemical Engineering Journal, 2021, 407, 127960.	12.7	54
18	Facile Fabrication of Nylon66/Multi-Wall Carbon Nanotubes/Polyvinyl Alcohol Nanofiber Bundles for Use as Humidity Sensors. Journal of Macromolecular Science - Physics, 2021, 60, 368-380.	1.0	1

#	Article	IF	CITATIONS
19	An Ultrasensitive, Durable and Stretchable Strain Sensor with Crack-wrinkle Structure for Human Motion Monitoring. Chinese Journal of Polymer Science (English Edition), 2021, 39, 316-326.	3.8	26
20	Hollow-porous fibers for intrinsically thermally insulating textiles and wearable electronics with ultrahigh working sensitivity. Materials Horizons, 2021, 8, 1037-1046.	12.2	59
21	Alternating aligned conductive stripes in polypropylene film with remarkable anisotropy for sensing application. Sensors and Actuators B: Chemical, 2021, 330, 129370.	7.8	5
22	Environment Tolerant Conductive Nanocomposite Organohydrogels as Flexible Strain Sensors and Power Sources for Sustainable Electronics. Advanced Functional Materials, 2021, 31, 2101696.	14.9	179
23	Multi-functional and flexible helical fiber sensor for micro-deformation detection, temperature sensing and ammonia gas monitoring. Composites Part B: Engineering, 2021, 211, 108621.	12.0	35
24	Microribbon Structured Polyvinylidene Fluoride with High-Performance Piezoelectricity for Sensing Application. ACS Applied Polymer Materials, 2021, 3, 2411-2419.	4.4	15
25	Highly Thermally Conductive Graphene-Based Thermal Interface Materials with a Bilayer Structure for Central Processing Unit Cooling. ACS Applied Materials & amp; Interfaces, 2021, 13, 25325-25333.	8.0	39
26	Continuous fabrication of polyethylene microfibrilar bundles for wearable personal thermal management fabric. Applied Surface Science, 2021, 549, 149255.	6.1	28
27	Flexible and heat-resistant carbon nanotube/graphene/polyimide foam for broadband microwave absorption. Composites Science and Technology, 2021, 212, 108848.	7.8	28
28	Ultralight carbon nanotube/graphene/polyimide foam with heterogeneous interfaces for efficient electromagnetic interference shielding and electromagnetic wave absorption. Carbon, 2021, 176, 118-125.	10.3	122
29	Tunable and Nacreâ€Mimetic Multifunctional Electronic Skins for Highly Stretchable Contactâ€Noncontact Sensing. Small, 2021, 17, e2100542.	10.0	69
30	Green Production of Covalently Functionalized Boron Nitride Nanosheets via Saccharide-Assisted Mechanochemical Exfoliation. ACS Sustainable Chemistry and Engineering, 2021, 9, 11155-11162.	6.7	23
31	Highly linear and low hysteresis porous strain sensor for wearable electronic skins. Composites Communications, 2021, 26, 100809.	6.3	33
32	A Healable and Mechanically Enhanced Composite with Segregated Conductive Network Structure for High-Efficient Electromagnetic Interference Shielding. Nano-Micro Letters, 2021, 13, 162.	27.0	62
33	Bioinspired Multifunctional Photonicâ€Electronic Smart Skin for Ultrasensitive Health Monitoring, for Visual and Selfâ€Powered Sensing. Advanced Materials, 2021, 33, e2102332.	21.0	107
34	Low-temperature carbonized carbon nanotube/cellulose aerogel for efficient microwave absorption. Composites Part B: Engineering, 2021, 220, 108985.	12.0	95
35	Highly stretchable and durable fibrous strain sensor with growth ring-like spiral structure for wearable electronics. Composites Part B: Engineering, 2021, 225, 109275.	12.0	27
36	Facile heteroatom doping of biomass-derived carbon aerogels with hierarchically porous architecture and hybrid conductive network: Towards high electromagnetic interference shielding effectiveness and high absorption coefficient. Composites Part B: Engineering, 2021, 224, 109175.	12.0	50

#	Article	IF	CITATIONS
37	Ultra-stretchable and multifunctional wearable electronics for superior electromagnetic interference shielding, electrical therapy and biomotion monitoring. Journal of Materials Chemistry A, 2021, 9, 7238-7247.	10.3	65
38	Superior actuation performance and healability achieved in a transparent, highly stretchable dielectric elastomer film. Journal of Materials Chemistry C, 2021, 9, 12239-12247.	5.5	13
39	Tribological Properties of Self-Lubricating Thermoplastic Polyurethane/Oil-Loaded Microcapsule Composites Based on Melt Processing. Industrial & Engineering Chemistry Research, 2021, 60, 16023-16031.	3.7	4
40	Nacre-inspired tunable strain sensor with synergistic interfacial interaction for sign language interpretation. Nano Energy, 2021, 90, 106606.	16.0	39
41	Flexible and wearable carbon black/thermoplastic polyurethane foam with a pinnate-veined aligned porous structure for multifunctional piezoresistive sensors. Chemical Engineering Journal, 2020, 382, 122985.	12.7	153
42	Transparent Conductive Flexible Trilayer Films for a Deicing Window and Self-Recover Bending Sensor Based on a Single-Walled Carbon Nanotube/Polyvinyl Butyral Interlayer. ACS Applied Materials & Interfaces, 2020, 12, 1454-1464.	8.0	27
43	High-Performance Wearable Strain Sensor Based on Graphene/Cotton Fabric with High Durability and Low Detection Limit. ACS Applied Materials & Interfaces, 2020, 12, 1474-1485.	8.0	125
44	Multifunctional stretchable strain sensor based on polydopamine/ reduced graphene oxide/ electrospun thermoplastic polyurethane fibrous mats for human motion detection and environment monitoring. Composites Part B: Engineering, 2020, 183, 107696.	12.0	104
45	Ultra-sensitive and durable strain sensor with sandwich structure and excellent anti-interference ability for wearable electronic skins. Composites Science and Technology, 2020, 200, 108448.	7.8	85
46	An electrically conductive polymer composite with a co-continuous segregated structure for enhanced mechanical performance. Journal of Materials Chemistry C, 2020, 8, 11546-11554.	5.5	40
47	Large-area fabrication and applications of patterned surface with anisotropic superhydrophobicity. Applied Surface Science, 2020, 529, 147027.	6.1	25
48	Steric stabilizer-based promotion of uniform polyaniline shell for enhanced electromagnetic wave absorption of carbon nanotube/polyaniline hybrids. Composites Part B: Engineering, 2020, 199, 108309.	12.0	36
49	Flexible conductive polymer composites for smart wearable strain sensors. SmartMat, 2020, 1, e1010.	10.7	119
50	Highly Stretchable Sheath–Core Yarns for Multifunctional Wearable Electronics. ACS Applied Materials & Interfaces, 2020, 12, 29717-29727.	8.0	20
51	Self-assembled reduced graphene oxide/nickel nanofibers with hierarchical core-shell structure for enhanced electromagnetic wave absorption. Carbon, 2020, 167, 530-540.	10.3	80
52	Superior and highly absorbed electromagnetic interference shielding performance achieved by designing the reflection-absorption-integrated shielding compartment with conductive wall and lossy core. Chemical Engineering Journal, 2020, 393, 124644.	12.7	87
53	Facile Construction of a Superhydrophobic Surface on a Textile with Excellent Electrical Conductivity and Stretchability. Industrial & Engineering Chemistry Research, 2020, 59, 7546-7553.	3.7	25
54	Ultra-Stretchable, durable and conductive hydrogel with hybrid double network as high performance strain sensor and stretchable triboelectric nanogenerator. Nano Energy, 2020, 76, 105035.	16.0	209

#	Article	IF	CITATIONS
55	Spontaneous exfoliation and tailoring derived oxygen-riched porous carbon nanosheets for superior Li+ storage performance. Chemical Engineering Journal, 2020, 387, 124104.	12.7	30
56	Highly stretchable and durable fiber-shaped strain sensor with porous core-sheath structure for human motion monitoring. Composites Science and Technology, 2020, 189, 108038.	7.8	81
57	Lightweight and Robust Carbon Nanotube/Polyimide Foam for Efficient and Heat-Resistant Electromagnetic Interference Shielding and Microwave Absorption. ACS Applied Materials & Interfaces, 2020, 12, 8704-8712.	8.0	227
58	Ultra-stretchable triboelectric nanogenerator as high-sensitive and self-powered electronic skins for energy harvesting and tactile sensing. Nano Energy, 2020, 70, 104546.	16.0	171
59	Asymmetric conductive polymer composite foam for absorption dominated ultra-efficient electromagnetic interference shielding with extremely low reflection characteristics. Journal of Materials Chemistry A, 2020, 8, 9146-9159.	10.3	196
60	Ultraâ€Stretchable Porous Fiberâ€Shaped Strain Sensor with Exponential Response in Full Sensing Range and Excellent Antiâ€Interference Ability toward Buckling, Torsion, Temperature, and Humidity. Advanced Electronic Materials, 2019, 5, 1900538.	5.1	63
61	Amorphous MnSiO3 confined in graphene sheets for superior lithium-ion batteries. Journal of Alloys and Compounds, 2019, 804, 243-251.	5.5	20
62	Highly Stretchable, Transparent, and Bioâ€Friendly Strain Sensor Based on Selfâ€Recovery Ionicâ€Covalent Hydrogels for Human Motion Monitoring. Macromolecular Materials and Engineering, 2019, 304, 1900227.	3.6	71
63	Interfacial adhesion enhanced flexible polycarbonate/carbon nanotubes transparent conductive film for vapor sensing. Composites Communications, 2019, 15, 80-86.	6.3	21
64	Ultrathin, flexible transparent Joule heater with fast response time based on single-walled carbon nanotubes/poly(vinyl alcohol) film. Composites Science and Technology, 2019, 183, 107796.	7.8	77
65	Facile fabrication of triboelectric nanogenerator based on low-cost thermoplastic polymeric fabrics for large-area energy harvesting and self-powered sensing. Nano Energy, 2019, 65, 104068.	16.0	89
66	A Highly Sensitive and Stretchable Yarn Strain Sensor for Human Motion Tracking Utilizing a Wrinkle-Assisted Crack Structure. ACS Applied Materials & Interfaces, 2019, 11, 36052-36062.	8.0	141
67	Highly Stretchable and Sensitive Strain Sensor with Porous Segregated Conductive Network. ACS Applied Materials & Interfaces, 2019, 11, 37094-37102.	8.0	116
68	Smart strain sensing organic–inorganic hybrid hydrogels with nano barium ferrite as the cross-linker. Journal of Materials Chemistry C, 2019, 7, 2353-2360.	5.5	142
69	Significant Stretchability Enhancement of a Crack-Based Strain Sensor Combined with High Sensitivity and Superior Durability for Motion Monitoring. ACS Applied Materials & Interfaces, 2019, 11, 7405-7414.	8.0	243
70	Anisotropic Conductive Polymer Composites Based on High Density Polyethylene/Carbon Nanotube/Polyoxyethylene Mixtures for Microcircuits Interconnection and Organic Vapor Sensor. ACS Applied Nano Materials, 2019, 2, 3636-3647.	5.0	30
71	Multifunctional flexible carbon black/polydimethylsiloxane piezoresistive sensor with ultrahigh linear range, excellent durability and oil/water separation capability. Chemical Engineering Journal, 2019, 372, 373-382.	12.7	146
72	A super-stretchable and tough functionalized boron nitride/PEDOT:PSS/poly(<i>N</i> -isopropylacrylamide) hydrogel with self-healing, adhesion, conductive and photothermal activity. Journal of Materials Chemistry A, 2019, 7, 8204-8209.	10.3	101

#	Article	IF	CITATIONS
73	Design of Helically Double-Leveled Gaps for Stretchable Fiber Strain Sensor with Ultralow Detection Limit, Broad Sensing Range, and High Repeatability. ACS Applied Materials & Interfaces, 2019, 11, 4345-4352.	8.0	91
74	Electrically conductive carbon black/electrospun polyamide 6/poly(vinyl alcohol) composite based strain sensor with ultrahigh sensitivity and favorable repeatability. Materials Letters, 2019, 236, 60-63.	2.6	39
75	Remarkably anisotropic conductive MWCNTs/polypropylene nanocomposites with alternating microlayers. Chemical Engineering Journal, 2019, 358, 924-935.	12.7	70
76	Tunable temperature-resistivity behaviors of carbon black/polyamide 6 /high-density polyethylene composites with conductive electrospun PA6 fibrous network. Journal of Composite Materials, 2019, 53, 1897-1906.	2.4	8
77	Highly stretchable and durable strain sensor based on carbon nanotubes decorated thermoplastic polyurethane fibrous network with aligned wave-like structure. Chemical Engineering Journal, 2019, 360, 762-777.	12.7	190
78	Thermo-compression-aligned functional graphene showing anisotropic response to in-plane stretching and out-of-plane bending. Journal of Materials Science, 2018, 53, 6574-6585.	3.7	17
79	A highly stretchable and stable strain sensor based on hybrid carbon nanofillers/polydimethylsiloxane conductive composites for large human motions monitoring. Composites Science and Technology, 2018, 156, 276-286.	7.8	276
80	Vapor sensing performance as a diagnosis probe to estimate the distribution of multi-walled carbon nanotubes in poly(lactic acid)/polypropylene conductive composites. Sensors and Actuators B: Chemical, 2018, 255, 2809-2819.	7.8	41
81	Flexible electrically resistive-type strain sensors based on reduced graphene oxide-decorated electrospun polymer fibrous mats for human motion monitoring. Carbon, 2018, 126, 360-371.	10.3	367
82	Continuously prepared highly conductive and stretchable SWNT/MWNT synergistically composited electrospun thermoplastic polyurethane yarns for wearable sensing. Journal of Materials Chemistry C, 2018, 6, 2258-2269.	5.5	376
83	Segregated conductive polymer composite with synergistically electrical and mechanical properties. Composites Part A: Applied Science and Manufacturing, 2018, 105, 68-77.	7.6	55
84	Electrically conductive polymer composites for smart flexible strain sensors: a critical review. Journal of Materials Chemistry C, 2018, 6, 12121-12141.	5.5	522
85	Bioinspired Concentric-Cylindrical Multilayered Scaffolds with Controllable Architectures: Facile Preparation and Biological Applications. ACS Applied Materials & Interfaces, 2018, 10, 43512-43522.	8.0	20
86	Lightweight, mechanical robust foam with a herringbone-like porous structure for oil/water separation and filtering. Polymer Testing, 2018, 72, 86-93.	4.8	14
87	Ultrastretchable Multilayered Fiber with a Hollow-Monolith Structure for High-Performance Strain Sensor. ACS Applied Materials & Interfaces, 2018, 10, 34592-34603.	8.0	81
88	A highly stretchable carbon nanotubes/thermoplastic polyurethane fiber-shaped strain sensor with porous structure for human motion monitoring. Composites Science and Technology, 2018, 168, 126-132.	7.8	127
89	Aligned flexible conductive fibrous networks for highly sensitive, ultrastretchable and wearable strain sensors. Journal of Materials Chemistry C, 2018, 6, 6575-6583.	5.5	77
90	Segregated conductive CNTs/HDPE/UHMWPE composites fabricated by plunger type injection molding. Materials Letters, 2018, 229, 13-16.	2.6	26

#	Article	IF	CITATIONS
91	Revitalized βâ€form crystal during the remelting and recrystallization processes in isotactic polypropylene/glass fiber composites. Polymer Crystallization, 2018, 1, e10008.	0.8	2
92	Ultra-stretchable, sensitive and durable strain sensors based on polydopamine encapsulated carbon nanotubes/elastic bands. Journal of Materials Chemistry C, 2018, 6, 8160-8170.	5.5	131
93	Bridging the segregated structure in conductive polypropylene composites: An effective strategy to balance the sensitivity and stability of strain sensing performances. Composites Science and Technology, 2018, 163, 18-25.	7.8	30
94	Superhydrophobic Shish-kebab Membrane with Self-Cleaning and Oil/Water Separation Properties. ACS Sustainable Chemistry and Engineering, 2018, 6, 9866-9875.	6.7	147
95	Continuously fabricated transparent conductive polycarbonate/carbon nanotube nanocomposite films for switchable thermochromic applications. Journal of Materials Chemistry C, 2018, 6, 8360-8371.	5.5	79
96	Mechanical enhancement of melt-stretched β-nucleated isotactic polypropylene: The role of lamellar branching of β-crystal. Polymer Testing, 2017, 58, 227-235.	4.8	69
97	Strain sensing behaviors of epoxy nanocomposites with carbon nanotubes under cyclic deformation. Polymer, 2017, 112, 1-9.	3.8	94
98	Comparative assessment of the strain-sensing behaviors of polylactic acid nanocomposites: reduced graphene oxide or carbon nanotubes. Journal of Materials Chemistry C, 2017, 5, 2318-2328.	5.5	236
99	A tunable strain sensor based on a carbon nanotubes/electrospun polyamide 6 conductive nanofibrous network embedded into poly(vinyl alcohol) with self-diagnosis capabilities. Journal of Materials Chemistry C, 2017, 5, 4408-4418.	5.5	98
100	Continuous fabrication of polymer microfiber bundles with interconnected microchannels for oil/water separation. Applied Materials Today, 2017, 9, 77-81.	4.3	84
101	Conductive thermoplastic polyurethane composites with tunable piezoresistivity by modulating the filler dimensionality for flexible strain sensors. Composites Part A: Applied Science and Manufacturing, 2017, 101, 41-49.	7.6	155
102	The effect of filler dimensionality on the electromechanical performance of polydimethylsiloxane based conductive nanocomposites for flexible strain sensors. Composites Science and Technology, 2017, 139, 64-73.	7.8	300
103	Conductive Nanocomposites: Positive Temperature Coefficient (PTC) Evolution of Segregated Structural Conductive Polypropylene Nanocomposites with Visually Traceable Carbon Black Conductive Network (Adv. Mater. Interfaces 17/2017). Advanced Materials Interfaces, 2017, 4, .	3.7	0
104	Heating-induced negative temperature coefficient effect in conductive graphene/polymer ternary nanocomposites with a segregated and double-percolated structure. Journal of Materials Chemistry C, 2017, 5, 8233-8242.	5.5	66
105	Positive Temperature Coefficient (PTC) Evolution of Segregated Structural Conductive Polypropylene Nanocomposites with Visually Traceable Carbon Black Conductive Network. Advanced Materials Interfaces, 2017, 4, 1700265.	3.7	30
106	Flexible and Lightweight Pressure Sensor Based on Carbon Nanotube/Thermoplastic Polyurethane-Aligned Conductive Foam with Superior Compressibility and Stability. ACS Applied Materials & Interfaces, 2017, 9, 42266-42277.	8.0	225
107	Conductive herringbone structure carbon nanotube/thermoplastic polyurethane porous foam tuned by epoxy for high performance flexible piezoresistive sensor. Composites Science and Technology, 2017, 149, 166-177.	7.8	99
108	A flexible and self-formed sandwich structure strain sensor based on AgNW decorated electrospun fibrous mats with excellent sensing capability and good oxidation inhibition properties. Journal of Materials Chemistry C, 2017, 5, 7035-7042.	5.5	100

#	Article	IF	CITATIONS
109	Lightweight conductive graphene/thermoplastic polyurethane foams with ultrahigh compressibility for piezoresistive sensing. Journal of Materials Chemistry C, 2017, 5, 73-83.	5.5	576
110	Simultaneously improving tensile strength and toughness of meltâ€spun βâ€nucleated isotactic polypropylene fibers. Journal of Applied Polymer Science, 2016, 133, .	2.6	5
111	Piezoresistive behavior of porous carbon nanotube-thermoplastic polyurethane conductive nanocomposites with ultrahigh compressibility. Applied Physics Letters, 2016, 108, .	3.3	102
112	Organic vapor sensing behaviors of conductive thermoplastic polyurethane–graphene nanocomposites. Journal of Materials Chemistry C, 2016, 4, 4459-4469.	5.5	198
113	Electrically conductive strain sensing polyurethane nanocomposites with synergistic carbon nanotubes and graphene bifillers. Nanoscale, 2016, 8, 12977-12989.	5.6	464
114	Electrically conductive thermoplastic polyurethane/polypropylene nanocomposites with selectively distributed graphene. Polymer, 2016, 97, 11-19.	3.8	159
115	Carbon Nanotubes-Adsorbed Electrospun PA66 Nanofiber Bundles with Improved Conductivity and Robust Flexibility. ACS Applied Materials & Interfaces, 2016, 8, 14150-14159.	8.0	241
116	Liquid sensing behaviors of conductive polypropylene composites containing hybrid fillers of carbon fiber and carbon black. Composites Part B: Engineering, 2016, 94, 45-51.	12.0	29
117	Interfacial interaction enhancement by shear-induced β-cylindrite in isotactic polypropylene/glass fiber composites. Polymer, 2016, 100, 111-118.	3.8	54
118	Annealing Induced Mechanical Reinforcement of Injection Molded iPP Parts. Macromolecular Materials and Engineering, 2016, 301, 1468-1472.	3.6	38
119	Particle size induced tunable positive temperature coefficient characteristics in electrically conductive carbon nanotubes/polypropylene composites. Materials Letters, 2016, 182, 314-317.	2.6	26
120	Liquid-sensing behaviors of carbon black/polyamide 6/high-density polyethylene composite containing ultrafine conductive electrospun fibrous network. Colloid and Polymer Science, 2016, 294, 1343-1350.	2.1	8
121	The role of conductive pathways in the conductivity and rheological behavior of poly(methyl) Tj ETQq1 1 0.7843	.4 rgBT /O	verlock 10
122	Mechanically Strengthened Polyamide 66 Nanofibers Bundles via Compositing With Polyvinyl Alcohol. Macromolecular Materials and Engineering, 2016, 301, 212-219.	3.6	12
123	Electrically conductive thermoplastic elastomer nanocomposites at ultralow graphene loading levels for strain sensor applications. Journal of Materials Chemistry C, 2016, 4, 157-166.	5.5	484
124	Microstructure and Mechanical Properties of Isotactic Polypropylene Films Fabricated via Melt-Extrusion and Uniaxial-Stretching. Journal of Macromolecular Science - Physics, 2016, 55, 158-174.	1.0	6
125	Tailoring microstructure and mechanical properties of injection molded isotactic–polypropylene via high temperature preshear. Polymer Engineering and Science, 2015, 55, 2714-2721.	3.1	9
126	Tuning of vapor sensing behaviors of eco-friendly conductive polymer composites utilizing ramie fiber. Sensors and Actuators B: Chemical, 2015, 221, 1279-1289.	7.8	64

#	Article	IF	CITATIONS
127	Tunable resistivity–temperature characteristics of an electrically conductive multi-walled carbon nanotubes/epoxy composite. Materials Letters, 2015, 159, 276-279.	2.6	12
128	Shear-induced interfacial sheath structure in isotactic polypropylene/glass fiber composites. Polymer, 2015, 70, 326-335.	3.8	32
129	Enhancing oriented crystals in injection-molded HDPE through introduction of pre-shear. Materials & Design, 2015, 78, 12-18.	5.1	19
130	Fabrication of a polymer/aligned shish-kebab composite: microstructure and mechanical properties. RSC Advances, 2015, 5, 60392-60400.	3.6	12
131	Suppressing the skin–core structure in injection-molded HDPE parts via the combination of pre-shear and UHMWPE. RSC Advances, 2015, 5, 84483-84491.	3.6	15
132	New insight into lamellar branching of β-nucleated isotactic polypropylene upon melt-stretching: WAXD and SAXS study. Journal of Materials Science, 2015, 50, 599-604.	3.7	25
133	Liquidâ€sensing behaviors of carbon black/polypropylene and carbon nanotubes/polypropylene composites: A comparative study. Polymer Composites, 2015, 36, 205-213.	4.6	8
134	Study on Impact Property and Fracture Morphology of Injection-molded Optical-grade Polycarbonate. Journal of Macromolecular Science - Physics, 2014, 53, 336-346.	1.0	1
135	Temperature-resistivity characteristics of a segregated conductive CB/PP/UHMWPE composite. Colloid and Polymer Science, 2014, 292, 2891-2898.	2.1	30
136	Tuning of the PTC and NTC effects of conductive CB/PA6/HDPE composite utilizing an electrically superfine electrospun network. Materials Letters, 2014, 132, 48-51.	2.6	32
137	Synergistic effect of carbon fibers on the conductive properties of a segregated carbon black/polypropylene composite. Materials Letters, 2014, 129, 72-75.	2.6	33
138	The strain-sensing behaviors of carbon black/polypropylene and carbon nanotubes/polypropylene conductive composites prepared by the vacuum-assisted hot compression. Colloid and Polymer Science, 2014, 292, 945-951.	2.1	18
139	Wide distribution of shish-kebab structure and tensile property of micro-injection-molded isotactic polypropylene microparts: a comparative study with injection-molded macroparts. Journal of Materials Science, 2014, 49, 1041-1048.	3.7	36
140	Electrically conductive CB/PA6/HDPE composite with a CB particles coated electrospun PA6 fibrous network. Materials Letters, 2014, 114, 96-99.	2.6	12
141	Liquid sensing properties of carbon black/polypropylene composite with a segregated conductive network. Sensors and Actuators A: Physical, 2014, 217, 13-20.	4.1	16
142	Pre-shear induced anomalous distribution of β-form in injection molded iPP. Polymer Testing, 2013, 32, 545-552.	4.8	23
143	Study of shear-induced interfacial crystallization in polymer-based composite through in situ monitoring interfacial shear stress. Journal of Materials Science, 2013, 48, 5354-5360.	3.7	12
144	Organic vapor sensing behaviors of carbon black/poly (lactic acid) conductive biopolymer composite. Colloid and Polymer Science, 2013, 291, 2871-2878.	2.1	28

#	Article	IF	CITATIONS
145	Crystalline Structure of Injection Molded β-Isotactic Polypropylene: Analysis of the Oriented Shear Zone. Industrial & Engineering Chemistry Research, 2013, 52, 11996-12002.	3.7	58
146	Comparative Study of Strain Sensing Behaviors of Carbon Black/Polypropylene and Carbon Nanotubes/Polypropylene with Different Tensile Speeds. Polymer-Plastics Technology and Engineering, 2013, 52, 1303-1307.	1.9	2
147	β-Crystal in the iPP melt encapsulated by transcrystallinity and spherulites: effect of molecular weight. Journal of Materials Science, 2013, 48, 2326-2333.	3.7	3
148	Realizing the simultaneously improved toughness and strength ofÂultra-thin LLDPE parts through annealing. Polymer, 2013, 54, 6843-6852.	3.8	24
149	Electrospun isotactic polypropylene fibers: Self-similar morphology and microstructure. Polymer, 2013, 54, 3117-3123.	3.8	19
150	Tuning of liquid sensing performance of conductive carbon black (CB)/polypropylene (PP) composite utilizing a segregated structure. Composites Part A: Applied Science and Manufacturing, 2013, 55, 11-18.	7.6	36
151	A comparison between strain sensing behaviors of carbon black/polypropylene and carbon nanotubes/polypropylene electrically conductive composites. Composites Part A: Applied Science and Manufacturing, 2013, 48, 129-136.	7.6	159
152	Nonlinear current-voltage characteristics of conductive polyethylene composites with carbon black filled pet microfibrils. Chinese Journal of Polymer Science (English Edition), 2013, 31, 211-217.	3.8	17
153	Unexpected molecular weight dependence of shish kebab in waterâ€assisted injection molded HDPE. Polymers for Advanced Technologies, 2013, 24, 270-272.	3.2	21
154	Enhanced βâ€crystal formation of isotactic polypropylene under the combined effects of acidâ€corroded glass fiber and preshear. Polymer Composites, 2013, 34, 1250-1260.	4.6	15
155	A Conductive Carbon Nanotube-Polymer Composite Based on a Co-continuous Blend. Journal of Macromolecular Science - Physics, 2013, 52, 167-177.	1.0	2
156	Organic liquid stimuliâ€response behaviors of electrically conductive microfibrillar composite with a selective conductive component distribution. Journal of Applied Polymer Science, 2012, 124, 4466-4474.	2.6	2
157	Electrical Properties of an Ultralight Conductive Carbon Nanotube/Polymer Composite Foam Upon Compression. Polymer-Plastics Technology and Engineering, 2012, 51, 304-306.	1.9	19
158	Enhanced orientation of the waterâ€assisted injectionâ€molded ipp in the presence of nucleating agent. Polymer Engineering and Science, 2012, 52, 725-732.	3.1	22
159	The hierarchical structure of waterâ€assisted injection molded high density polyethylene: Small angle Xâ€ray scattering study. Journal of Applied Polymer Science, 2012, 125, 2297-2303.	2.6	19
160	Anomalous attenuation and structural origin of positive temperature coefficient (PTC) effect in a carbon black (CB)/poly(ethylene terephthalate) (PET)/polyethylene (PE) electrically conductive microfibrillar polymer composite with a preferential CB distribution. Journal of Applied Polymer Science, 2012, 125, E561.	2.6	24
161	Transcrystallization in nanofiber bundle/isotactic polypropylene composites: effect of matrix molecular weight. Colloid and Polymer Science, 2012, 290, 1157-1164.	2.1	14
162	Temperature and time dependence of electrical resistivity in an anisotropically conductive polymer composite with <i>in situ</i> conductive microfibrils. Journal of Applied Polymer Science, 2012, 124, 1808-1814.	2.6	15

#	Article	IF	CITATIONS
163	Conductive network formation during annealing of an oriented polyethylene-based composite. Journal of Materials Science, 2012, 47, 3713-3719.	3.7	21
164	The Resistivity Response of an Anisotropically Conductive Polymer Composite with in-situ Conductive Microfibrils During Cooling. Polymer-Plastics Technology and Engineering, 2011, 50, 1511-1514.	1.9	10
165	Morphological comparison of isotactic polypropylene molded by water-assisted and conventional injection molding. Journal of Materials Science, 2011, 46, 7830-7838.	3.7	39
166	HDPE solution crystallization induced by electrospun PA66 nanofiber. Colloid and Polymer Science, 2011, 289, 843-848.	2.1	13
167	Negative effect of stretching on the development of βâ€phase in βâ€nucleated isotactic polypropylene. Polymer International, 2011, 60, 1016-1023.	3.1	9
168	Oriented structure in stretched isotactic polypropylene melt and its unexpected recrystallization: optical and Xâ€ray studies. Polymer International, 2011, 60, 1434-1441.	3.1	17
169	Electrical conductivity and major mechanical and thermal properties of carbon nanotubeâ€filled polyurethane foams. Journal of Applied Polymer Science, 2011, 120, 3014-3019.	2.6	77
170	Positive temperature coefficient and timeâ€dependent resistivity of carbon nanotubes (CNTs)/ultrahigh molecular weight polyethylene (UHMWPE) composite. Journal of Applied Polymer Science, 2009, 114, 1002-1010.	2.6	27
171	Electrically conductive in situ microfibrillar composite with a selective carbon black distribution: An unusual resistivity–temperature behavior upon cooling. Polymer, 2008, 49, 1037-1048.	3.8	58
172	Electrically conductive carbon black (CB) filled in situ microfibrillar poly(ethylene terephthalate) (PET)/polyethylene (PE) composite with a selective CB distribution. Polymer, 2007, 48, 849-859.	3.8	194
173	Anomalous attenuation of the positive temperature coefficient of resistivity in a carbon-black-filled polymer composite with electrically conductive in situ microfibrils. Applied Physics Letters, 2006, 89, 032105.	3.3	36